JACC: CARDIOVASCULAR IMAGING
VOL. 5, NO. 3, SUPPL S, 2012
© 2012 BY THE AMERICAN COLLEGE OF CARDIOLOGY FOUNDATION
ISSN 1936-878X/$36.00
PUBLISHED BY ELSEVIER INC.
DOI:10.1016/j.jcmg.2011.02.026

Relationship Between Palpography and Virtual Histology in Patients With Acute Coronary Syndromes

Salvatore Brugaletta, MD,*† Hector M. Garcia-Garcia, MD, PhD,*‡ Patrick W. Serruys, MD, PhD,* Akiko Maehara, MD,§ Vasim Farooq, MBChB,* Gary S. Mintz, MD,§ Bernard de Bruyne, MD,‖ Steven P. Marso, MD,¶ Stefan Verheye, MD, PhD,# Dariusz Dudek, MD,** Christian W. Hamm, MD,†† Nahim Farhat, MD,‡‡ Francois Schiele, MD,§§ John McPherson, MD,‖‖ Amir Lerman, MD,¶¶ Pedro R. Moreno, MD,## Bertil Wennerblom, MD,*** Martin Fahy, MSc,§ Barry Templin, MBA,††† Marie-Angel Morel, BSc,‡ Gerrit Anne van Es, PhD,§ Gregg W. Stone, MD§

Rotterdam, the Netherlands; New York, New York; Aalst and Antwerp, Belgium; Kansas City, Missouri; Krakow, Poland; Bad Nauheim, Germany; Elyria, Ohio; Besançon, France; Nashville, Tennessee; Rochester, Minnesota; Göteborg, Sweden; and Santa Clara, California

OBJECTIVES The purpose of this study was to correlate adverse events at long-term follow-up in patients after an acute coronary syndrome with coronary plaque characteristics derived from simultaneous evaluation of their mechanical and compositional properties using virtual histology (intravascular ultrasound virtual histology) and palpography.

BACKGROUND Fibroatheroma is the plaque morphology with the highest risk of causing adverse cardiac events. Palpography can potentially assess the local mechanical plaque properties with the possibility of identifying fibroatheroma with the highest risk of rupture.

METHODS A total of 114 patients with acute coronary syndrome from the PROSPECT (Providing Regional Observations to Study Predictors of Events in the Coronary Tree) trial underwent a single ultrasound imaging investigation of their 3 coronary vessels with the co-registration of intravascular ultrasound virtual histology and palpography. Major adverse cardiac events (MACE) (cardiac death, cardiac arrest, myocardial infarction, or unstable or progressive angina) were collected up to a median follow-up of 3.4 years and adjudicated to originally treated culprit versus untreated nonculprit lesions.

RESULTS In total, 488 necrotic core–rich plaques were identified and subclassified as thin-cap fibroatheroma (n = 111), calcified thick-cap fibroatheroma (n = 213), and noncalcified thick-cap fibroatheroma (n = 164) and matched to their co-registered palpography data. A total of 16 MACE, adjudicated to untreated nonculprit lesions, were recorded at follow-up. In patients in whom MACE developed, fibroatheroma were larger (plaque area 10.0 mm^2 [range: 8.4 to 11.6 mm^2] vs. 8.2 mm^2 [range: 7.7 to 8.8 mm^2] ($p = 0.03$) compared with patients who were MACE free. By palpography, the maximum and the density strain values did not differ between the varying subtypes of fibroatheroma of patients with or without MACE during follow-up.

CONCLUSIONS In acute coronary syndromes, patients treated with stents and contemporary pharmacotherapy, palpography did not provide additional diagnostic information for the identification of fibroatheroma with a high risk of rupture and MACE during long-term follow-up. (Providing Regional Observations to Study Predictors of Events in the Coronary Tree [PROSPECT]: An Imaging Study in Patients With Unstable Atherosclerotic Lesions; NCT00180466) (J Am Coll Cardiol Img 2012;5:S19–27)
© 2012 by the American College of Cardiology Foundation

From the *Erasmus University, Thoraxcentrum, Rotterdam, the Netherlands; †Thorax Institute, Department of Cardiology, Hospital Clinic, University of Barcelona, Spain; ‡Cardialysis, Rotterdam, the Netherlands; §Columbia University Medical

ABBREVIATIONS AND ACRONYMS

ACS = acute coronary syndromes

CSA = cross-sectional area

CTFA = calcified thick-cap fibroatheroma

EEM = external elastic membrane

hsCRP = high-sensitivity C-reactive protein

IVUS-VH = intravascular ultrasound virtual histology

IVUS = intravascular ultrasound

MACE = major adverse cardiac event(s)

NC = necrotic core

NCTFA = noncalcified thick-cap fibroatheroma

NSTEMI = non–ST-segment elevation myocardial infarction

ROC = Rotterdam classification

STEMI = ST-segment elevation myocardial infarction

TCFA = thin-cap fibroatheroma

VH = virtual histology

In the modern era of cardiology, the prevention of coronary events through identification of coronary plaques at high risk of events has become a topic of intense research. Several anatomopathologic studies previously showed that most atherosclerotic plaques responsible for acute coronary syndromes (ACS) are angiographically mild (1,2). The thrombosis associated with rupture of a thin-cap fibroatheroma (TCFA) is the most common cause of myocardial infarction and cardiac death (3–6). Moreover, the degree of mechanical strain exhibited by the plaque is related to the thickness of the cap (7,8).

See page S39

In patients with ACS recruited in the PROSPECT (Providing Regional Observations to Study Predictors of Events in the Coronary Tree) study (9–16), intravascular ultrasound virtual histology (IVUS-VH) demonstrated that the plaques responsible for major adverse cardiac events (MACE), at a median term follow-up of 3.4 years, had a larger plaque burden and smaller lumen area and/or were mostly virtual histology (VH) TCFAs.

IVUS palpography is a technique that can allow the assessment of local mechanical tissue properties, with previous in vitro studies suggesting a high sensitivity and specificity for detecting vulnerable plaques (17–19). In a subgroup of patients from the PROSPECT trial, in whom combined IVUS-VH and palpography recordings were performed, we explored the potential relationship between the mechanical and compositional properties of fibroatheromas and their prognostic value in predicting future cardiovascular events.

METHODS

Population. The study design of the PROSPECT trial has been published (9,10). Briefly, this multicenter, prospective, international study was designed to identify imaging and serologic predictors of vulnerable plaque events in patients who underwent percutaneous coronary intervention for ACS. After treatment of their culprit lesions, patients underwent 3-vessel gray-scale IVUS and IVUS-VH imaging of culprit and nonculprit arteries. The main inclusion criteria were: 1) acute cardiac pain or angina equivalent consistent with unstable angina or myocardial infarction lasting >10 min within the past 72 h; and 2) the presence of any of the following: increased biochemical markers of myocardial necrosis (creatine kinase-myocardial band isoenzyme or troponin I or T) greater than the upper limits of normal; ST-segment depression >1 mm in ≥2 contiguous leads or transient ST-segment elevation >1 mm in ≥2 contiguous leads lasting <30 min; or ST-segment elevation myocardial infarction with onset >24 h previously, diagnosed with the typical triad of nitrate-unresponsive chest pain lasting >30 min, ST-segment elevation >1 mm in ≥2 contiguous leads, or new left bundle branch block. This study was approved by the institutional review boards of the centers where the procedures were performed. Written informed consent was obtained from all patients before cardiac catheterization. Clinical follow-up was undertaken at 30 days, 6 months, and then yearly for at least 2 years. The study was terminated after all patients reached a 3-year follow-up.

Center/New York-Presbyterian Hospital and the Barcelona, Spain; Cardiovascular Research Foundation, New York, New York; ‖Cardiovascular Center, OLV Hospital, Aalst, Belgium; ¶Saint Luke's Mid America Heart Institute, University of Missouri-Kansas City, Kansas City, Missouri; #Antwerp Cardiovascular Institute Middelheim, Ziekenhuis Netwerk Antwerpen, Antwerp, Belgium; **Department of Cardiology, Jagiellonian University, Krakow, Poland; ††Kerckhoff Klinik, Bad Nauheim, Germany; ‡‡EMH Regional Medical Center, Elyria, Ohio; §§University Hospital Jean Minjoz, Besançon, France; |||Vanderbilt University Medical Center, Nashville, Tennessee; ¶¶Division of Cardiovascular Diseases, Department of Internal Medicine, Mayo Clinic and College of Medicine, Rochester, Minnesota; ##The Mount Sinai School of Medicine, New York, New York; ***Cardiology Department, Sahlgrenska University Hospital, Göteborg, Sweden; and †††Abbott Vascular, Santa Clara, California. The study was sponsored and funded by Abbott Vascular and Volcano Corporation. Dr. Maehara has received a research grant from Boston Scientific and lecture fees from Volcano. Dr. Mintz has received grant support, consulting fees, and honoraria from Volcano and Boston Scientific. Dr. Dudek has received research grants from or served as consultant/advisory board member for Abbott, Adamed, Biotronik, Balton, Bayer, BBraun, BioMatrix, Boston Scientific, Boehringer Ingelheim, Bristol-Myers Squibb, Cordis, Cook, Eli Lilly, EuroCor, Glaxo, Invatec, Medtronic, The Medicines Company, MSD, Nycomed, Orbus-Neich, Pfizer, Possis, Promed, Sanofi-Aventis, Siemens, Solvay, Terumo, and Tyco. Dr. McPherson is a consultant for Abbott Vascular. Dr. Stone has received research grants from Volcano and InfraReDx; and is on the scientific advisory board and receives honoraria from Boston Scientific and Abbott Vascular. All other authors have reported that they have no relationships relevant to the contents of this paper to disclose.

Manuscript received September 21, 2010; revised manuscript received December 16, 2010, accepted February 14, 2011.

Radiofrequency IVUS analysis. Radiofrequency IVUS of the left main and proximal 6 to 8 cm of each major epicardial coronary artery using a phased-array, 20-MHz, 3.2-F catheter (Eagle Eye, Volcano Corporation, Rancho Cordova, California) were performed. During motorized catheter pullback, at 0.5 mm/s, gray-scale IVUS was recorded, and raw radiofrequency data capture was gated to the R wave (In-Vision Gold, Volcano Corporation). Radiofrequency IVUS uses spectral (frequency) analysis as well as amplitude data from the IVUS signal, which has been correlated with histologic samples with high sensitivity and specificity (20,21).

All baseline IVUS images were prospectively offline analyzed at independent core laboratory without knowledge of subsequent events (Cardiovascular Research Foundation, New York, New York). Radiofrequency IVUS analyses were performed using: 1) QCU-CMS software (Medis, Leiden, the Netherlands) for contouring; 2) pcVH 2.1 software (Volcano Corporation) for contouring and data output; and 3) proprietary qVH software (Cardiovascular Research Foundation) for segmental qualitative assessment and quantitative data output. External elastic membrane (EEM) and lumen borders were contoured for all recorded frames (each ~0.4 mm in length). Quantitative IVUS measurements included EEM cross-sectional area (CSA), lumen CSA, plaque and media (EEM minus lumen) CSA, plaque burden (plaque and media divided by EEM CSA), and minimal lumen area. Radiofrequency IVUS plaque components were color coded as dense calcium (white), necrotic core (NC) (red), fibrofatty (light green), and fibrotic tissue (dark green) and reported as percentages of total plaque area. A lesion was defined as a segment with ≥3 consecutive frames with ≥40% plaque burden. Only the NC-rich plaques, FA, and TCFAs were considered in this study. Because calcium causes attenuation of the backscattering signal and may affect VH-IVUS plaque classification, the NC behind calcium is more likely to be artifactual. Consequently, the core laboratory separately categorized plaques with calcium according to its topographic distribution within the plaque. The NC-rich plaques were therefore classified as: 1) TCFA when the fibrous cap was absent; 2) calcified thick cap fibroatheroma (CTFA) when dense calcium

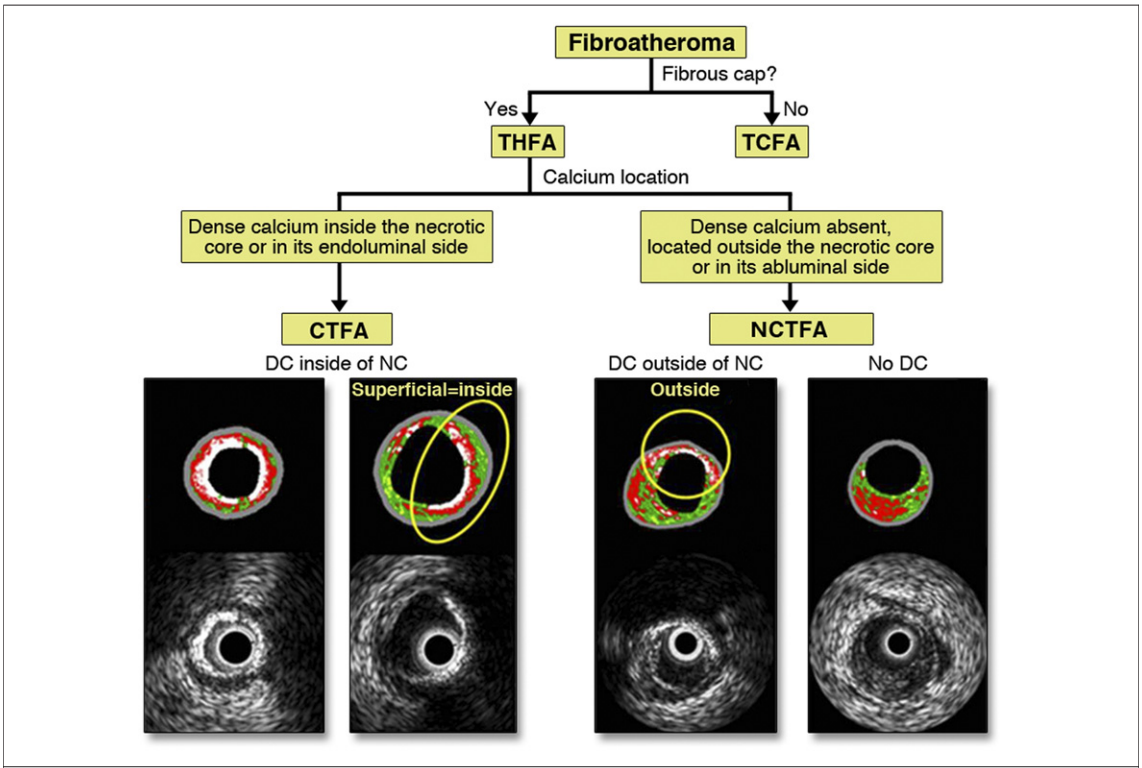

Figure 1. Subclassification of Fibroatheromas

Subclassification of fibroatheromas according to the presence of a fibrous cap and the topographic distribution of the dense calcium respect to the necrotic core. CTFA = calcified thick-cap fibroatheroma; DC = dense calcium; NC = necrotic core; NCTFA = noncalcified thick-cap fibroatheroma; TCFA = thin-cap fibroatheroma; THFA = thick-cap fibroatheroma.

was located within the NC or at its endoluminal side; 3) noncalcified TCFA (NCTFA) when dense calcium was absent or located outside the NC or on its abluminal side (22,23) (Fig. 1).

IVUS Palpography acquisition and analysis. IVUS palpography is a technique that allows the assessment of local mechanical tissue properties. At a defined pressure difference, soft-tissue (e.g., lipid-rich) components deform more than hard-tissue components (e.g., fibrous-calcified) (10–12). In coronary arteries, the tissue of interest is the vessel wall, whereas the blood pressure, with its physiologic changes during the heart cycle, is used as the excitation force. Radiofrequency data obtained at different pressure levels are compared to determine the local tissue deformation.

Each palpogram represents the strain information for a certain cross section over the full cardiac cycle. The longitudinal resolution of the acquisitions depends on heart rate and pullback speed. With a heart rate of 60 beats/min and a pullback speed of 1.0 mm/s, the longitudinal resolution is 1.0 mm. Palpograms were acquired simultaneously with radiofrequency IVUS using the same 20-MHz phased-array IVUS catheter. Digital radiofrequency data were acquired using a custom-designed workstation.

Data were acquired from the left main and proximal 6 to 8 cm of each major epicardial coronary artery at a pullback speed of 1.0 mm/s using an automated pullback device (Trak Back II, Volcano Corporation) with simultaneous recordings of the electrocardiogram, aortic pressure, and IVUS-VH data. The data were subsequently stored on a DVD and sent to the imaging core laboratory for offline analyses (Cardialysis BV, Rotterdam, the Netherlands). The local strain was calculated from the gated radiofrequency traces using cross-correlation analyses, displayed and color coded from blue (for 0% strain) through yellow (for 2% strain) via red, as previously described (19). This color-coded information was superimposed on the lumen vessel boundary of the cross-sectional IVUS image. Using previously described methodology, plaque strain values were assigned a Rotterdam classification (ROC) ranging from I to IV (ROC I, 0% to 0.5%; ROC II, 0.6% to <0.9%; ROC III, 0.9% to 1.2%; ROC IV, >1.2%) (8). A region was defined as a high-strain spot when it had high strain (ROC III to IV) that spanned an arc of at least 12° at the surface of a plaque (identified on the IVUS recording) adjacent to low-strain regions (<0.5%). The highest value of strain in the cross section was taken as the strain level of the spot.

Cross-correlation of the techniques. An independent experienced palpography analyst, blinded to the clinical information of all patients, used a color-blinded side-by-side view of both (palpography and IVUS-VH). Because the 2 recordings (electrocardiography-gated IVUS-VH, and nonelectrocardiography-gated palpography) were taken simultaneously from the same coronary region, the time stamps (i.e., time of acquisition) of both techniques were used to superimpose the palpography strain values over the coronary plaques identified by IVUS-VH (Fig. 2). Three different palpography endpoints for each plaque were then calculated.

1. Endpoint 1 (maximum strain value per plaque): maximum value of strain spots in the region of interest
2. Endpoint 2 (density of ROC III to IV per plaque): cumulative strain of the maximum strain in all ROC III/ROC IV high-strain spots, normalized by the number of cross sections
3. Endpoint 3 (density of ROC I/IV per plaque): cumulative strain of the maximum strain in all ROC I/ROC II/ROC III/ROC IV high-strain spots, normalized by the number of cross sections

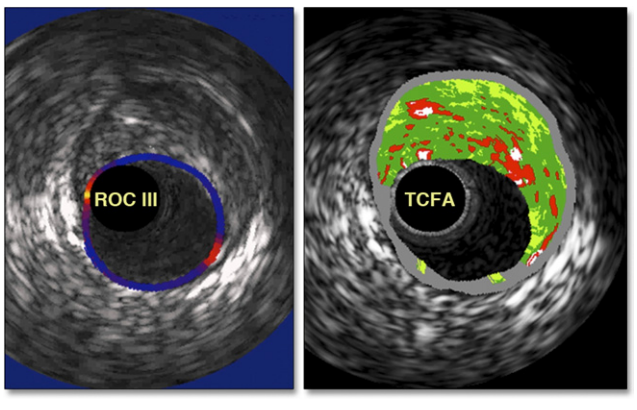

Figure 2. Palpography and IVUS-VH

Side-by-side view of palpography **(left)** and IVUS-VH **(right)** for a TCFA. High-strain spots on palpography are present at the edges of the plaque. Note that the time of acquisition of the images for both techniques is the same. IVUS-VH = intravascular ultrasound virtual histology; TCFA = thin-cap fibroatheroma.

Clinical endpoint definitions. The primary endpoint was MACE, defined as a composite of cardiac death, cardiac arrest, myocardial infarction, or unstable or progressive angina requiring rehospitalization or revascularization. On the basis of follow-up

angiography, MACE were adjudicated as occurring at the initially treated lesion site responsible for the original ACS (the index culprit lesion), or at previously untreated coronary segments (nonculprit lesions). If follow-up angiography was not performed, the location of the MACE was classified indeterminate (9,10).

Statistical analysis. Categorical variables are presented using frequencies and percentages, continuous variables with mean ± SD or median (interquartile range), according to their normal or non-normal distribution. Comparison and correlation among variables were done with different statistical tests according to their distribution. Analysis of normality of the continuous variables was performed with the Kolmogorov-Smirnov test. In particular, comparison among groups for variables normally distributed was performed by analysis of variance and for variables non-normally distributed by the Mann-Whitney or Kruskal-Wallis test. Correlation among variables was done by the Pearson or Spearman test, accordingly to their normal or non-normal distribution, respectively. Palpography endpoints were compared at the plaque level and at the patient level. To relate high-sensitivity C-reactive protein (hsCRP) values to plaque type, because hsCRP is patient specific, each patient was entered in the analysis, according to his or her worst plaque (TCFA, CTFA, or NCTFA). For plaque (i.e., fibroatheroma) or lesion level data, a model with a generalized estimating equations approach was used to compensate for any potential cluster effect of multiple plaques in the same lesion or multiple lesions in the same patient and presented as least-square means with 95% confidential intervals. A 2-sided p value <0.05 indicated statistical significance. Statistical analyses were performed using SPSS software version 13.0 (SPSS Inc., Chicago, Illinois).

RESULTS

Baseline clinical characteristics. Between October 29, 2004, and June 8, 2006, the PROSPECT trial enrolled 697 patients. In a subgroup of 114 patients, IVUS palpography and radiofrequency recordings were simultaneously obtained during a single IVUS pullback. Clinical baseline characteristics are shown in Table 1. At a median follow-up of 3.4 years, a total of 16 MACE were recorded in this population, adjudicated to untreated nonculprit lesions. Because no death or acute myocardial infarction in this subgroup occurred during follow-up, MACE therefore consisted mainly of new occurrences of unstable or progressive angina requiring rehospitalization or revascularization.

Table 1. Patient Characteristics, Baseline Laboratory Results, and Index Procedure

Age, yrs	55.7 ± 10.9
Female	25/114 (22)
Diabetes mellitus	13/114 (11.4)
Requiring insulin	3/114 (2.6)
Metabolic syndrome	31/114 (27.1)
Current cigarette use	65/114 (57.7)
Hypertension	56/114 (49.1)
Hyperlipidemia	62/114 (54.3)
Previous myocardial infarction	12/114 (10.5)
Family history of coronary artery disease	61/114 (53.5)
Framingham risk score	6.3 ± 3.1
Previous percutaneous coronary intervention	11/114 (9.6)
Clinical presentation	
ST-segment elevation myocardial infarction	44/114 (38.5)
Non–ST-segment elevation myocardial infarction	56/114 (49.3)
Unstable angina with electrocardiographic changes	14/114 (12.2)
Body mass index, kg/m^2	28.3 ± 5.1
Cholesterol, mg/dl	
Total	172.7 ± 42.5
LDL	81.4 ± 48.4
HDL	43.3 ± 21.1
Triglycerides, mg/dl,	128.8 ± 84.3
Hemoglobin A_{1c}, %,	5.8 (5.3–6.1)
Estimated creatinine clearance, ml/min	104.0 (79.0–132.4)
High-sensitivity C-reactive protein, mg/l	7.0 (2.4–16.6)

Values are mean ± SD, n (%), or median (interquartile range).
HDL = high-density lipoprotein; LDL = low-density lipoprotein.

Imaging analysis. A total of 488 NC-rich plaques were identified by radiofrequency IVUS and palpog-

Table 2. Lesion Characterization of Necrotic Core–Rich Plaques (N = 488)

Lumen cross-sectional area, mm^2	7.6 ± 3.2
External elastic membrane area, mm^2	16.2 ± 5.5
Plaque cross-sectional area, mm^2	8.6 ± 3.2
Plaque burden, %	53.5 ± 9.6
≥70%	37 (7.5)
Fibroatheroma length, mm	1.7 (0.9–3.0)
Tissue composition, %	
Fibrotic	29.5 ± 8.1
Fibrofatty	6.7 ± 4.4
Dense calcium	7.0 ± 4.7
Necrotic core	14.1 ± 4.8
Plaque classification	
Thin-cap fibroatheroma	111 (22.8)
Calcified thick-cap fibroatheroma	213 (43.6)
Noncalcified thick-cap fibroatheroma	164 (33.6)

Values are mean ± SD, n (%), or median (interquartile range).

Table 3. Palpography Analysis

	TCFA (n = 111)	CTFA (n = 213)	NCTFA (n = 164)	p Value
Maximum strain value (endpoint #1), %	0.56 ± 0.36	0.53 ± 0.44	0.58 ± 0.44	0.50
	0.45 (0.30–0.70)	0.40 (0.30–0.80)	0.50 (0.30–0.70)	
Density of ROC III–IV (endpoint #2), ROC/mm	0.08 ± 0.18	0.09 ± 0.27	0.08±0.20	0.80
	0.00 (0.00–0.00)	0.00 (0.00–0.00)	0.00 (0.00–0.00)	
Density of ROC I–IV (endpoint #3), ROC/mm	0.31 ± 0.20	0.33 ± 0.29	0.33 ± 0.27	0.70
	0.28 (0.15–0.40)	0.25 (0.15–0.42)	0.25 (0.15–0.44)	

Values are mean ± SD and median (interquartile range).
CTFA = calcified thick-cap fibroatheroma; NCTFA= noncalcified thick-cap fibroatheroma; ROC = Rotterdam classification; TCFA = thin-cap fibroatheroma.

raphy (4.2 per patient). Table 2 shows all imaging data. In particular, 22.8% were classified as TCFAs, 43.6% CTFAs, and 33.6% NCTFAs. No differences were found in palpography endpoints among these 3 types of plaque (Table 3).

The hsCRP values did not differ among the different types of plaque considered at the patient level (TCFA, 8.5 mg/l [interquartile range: 3.0 to 12.4 mg/l]; CTFA, 6.9 mg/l [interquartile range: 2.8 to 19.4 mg/l]; NCTFA, 8.5 mg/l [interquartile range: 4.0 to 19.7 mg/l]; p = 0.2). No correlation was found between palpography endpoints and hsCRP at the patient level (r = −0.004, p = 0.975 for endpoint #1; r = 0.073, p = 0.511 for endpoint #2; r = −0.46, p = 0.678 for endpoint #3). Palpography endpoint #1 was higher in patients with a clinical presentation of ST-segment elevation myocardial infarction (STEMI) or non–ST-segment elevation myocardial infarction (NSTEMI) compared with patients with unstable angina (0.31% [interquartile range: 0.25% to 0.50%]); NSTEMI (0.60% [interquartile range: 0.37% to 0.70%]); or STEMI (0.50% [interquartile range: 0.32% to 0.76%]) (Fig. 3). hsCRP values did not differ according to the clinical presentation (unstable angina, 4.5 mg/l [interquartile range: 2.6 to 10.5 mg/l] vs. NSTEMI, 6.6 mg/l [interquartile range: 2.6 to 12.4 mg/l] vs. STEMI, 9.1 mg/l [interquartile range: 2.2 to 20.7 mg/l]; p = 0.418). Comparison of the tertiles of endpoint 1 in terms of hsCRP values showed no differences among them (7.9 mg/l [interquartile range: 3.6 to 13.0 mg/l] vs. 6.6 mg/l [interquartile range: 1.6 to 11.1 mg/l] vs. 8.5 mg/ml [interquartile range: 2.4 to 18.0 mg/l], respectively; p = 0.794). The other palpography endpoints did not differ among patients according to their clinical presentation.

Plaques with ROC III to IV showed no differences compared with plaques with ROC I to II (Table 4). A weak correlation was found between

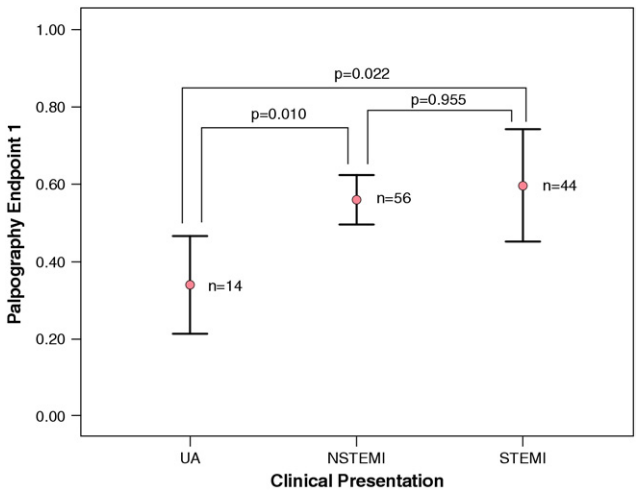

Figure 3. Maximum Strain Value Distribution According to Clinical Presentation

The mean of the maximum strain value (endpoint #1) in the necrotic core–rich plaques by clinical presentation. NSTEMI = non–ST-segment elevation myocardial infarction; STEMI = ST-segment elevation myocardial infarction; UA = unstable angina.

Table 4. Comparison of Radiofrequency IVUS Parameters and ROC Palpography Classification

IVUS-VH	ROC I–II Plaques (n = 404)	ROC III–IV Plaques (n = 84)	p Value
Plaque area, mm^2	8.5 (8.0–9.0)	8.2 (7.3–9.1)	0.40
Dense calcium, %	6.3 (5.6–7.0)	6.2 (5.1–7.2)	0.86
Necrotic core, %	12.9 (12.1–13.6)	12.5 (11.5–13.5)	0.44
Fibrous tissue, %	30.2 (28.9–31.4)	29.3 (27.1–31.5)	0.59
Fibrofatty tissue, %	7.2 (6.5–8.0)	7.53 (6.3–8.6)	0.59

All values are presented as generalized estimating equation–adjusted least mean square (95% confidence interval).
IVUS = intravascular ultrasound; IVUS-VH = intravascular ultrasound virtual histology; ROC = Rotterdam classification.

the palpography endpoint 3 and relative content of fibrous tissue for the TCFA plaques ($r = -0.2$, $p = 0.02$). No correlation was found between the other palpography endpoints and VH component for other VH plaque type (CTFA and NCTFA).

The fibroatheromas identified in the patients in whom MACE developed during follow-up were 49 of 488 (10.0%): TCFA, 11 of 49 (22.4%); CTFA, 22 of 49 (45%), and NCTFA, 16 of 49 (32.6%). These plaques demonstrated higher areas ($p = 0.03$) and a higher fibrofatty component ($p < 0.01$) compared with plaques of patients who were MACE free during follow-up (Table 5). However, in this substudy, no differences were found among the groups according to the distribution of VH plaque classification. No differences were found in palpography endpoints between the plaques of patients with or without MACE during follow-up (Table 5).

DISCUSSION

The principal findings of this substudy are the following: 1) larger fibroatheromas are confirmed to be more frequent in patients in whom cardiac events develop during long-term follow-up; and 2) palpography does not provide any additional diagnostic information with respect to the VH and does not specifically identify plaques at higher risk of events.

The PROSPECT study was the first trial to study atherosclerosis using a multimodality intracoronary imaging approach in patients after successfully treated ACS. This demonstrated that nonculprit lesions with a higher plaque burden and a radiofrequency IVUS morphology of TCFA were independent predictors of cardiovascular events over a 3-year follow-up period (9,11–16).

In our substudy, we focused on NC-rich plaques and analyzed the palpography data of these plaques. As shown in the main study, we found that larger fibroatheromas were more frequent in patients in whom events developed during follow-up. It is noteworthy to consider that, because previous studies demonstrated a correlation between plaque size and its NC content (24,25), use of gray-scale IVUS could be sufficiently powerful to identify larger and NC-rich plaques. In this substudy, no difference, indeed, was demonstrated in VH plaque distribution between plaques of patients in whom MACE developed during follow-up and those who were MACE free.

Palpography was previously shown to potentially detect differences in deformability (strain) exhibited by different types of plaques, with lipid-rich plaques deforming more and thus showing a higher strain value compared with calcified or fibrous plaques (17,19). Rodriguez-Granillo et al. (8) showed that IVUS-VH had an acceptable sensitivity to detect high strain as assessed by palpography, but a low specificity. However, all of these studies were performed retrospectively and could not identify the predictive value of these techniques in the detection of high-risk plaques. In our subanalysis of the PROSPECT trial, palpography analyses of all 3 coronary vessels were performed and all data were matched to each NC-rich plaque. Our approach was therefore plaque based, whereas Rodriguez-Granillo et al. (8) used a frame-based approach.

Using this plaque-based approach, we found that ROC III to IV plaques did not exhibit any difference in VH composition compared with ROC I to II plaques, confirming the results of our previous frame-based approach (8). In addition, palpography was already validated in an ex vivo model to identify thin-capped fibroatheromas. However, in this substudy, the strain values were found to be no different between plaques with a thin or a thick fibrous cap, as evaluated by IVUS (19,26,27).

The number of high-strain spots in the culprit epicardial vessel was previously found to be correlated with clinical presentation and significantly decrease with standard medical therapy (18). In our analysis, we confirmed that the high-strain spot can be correlated with the clinical presentation, finding a higher maximum strain value in patients with a clinical presentation of NSTEMI or STEMI compared with those with unstable angina (18) (Fig. 3). However, we did not achieve any correlation between the high-strain spot and

Table 5. Comparison of Coronary Plaques in Patients With and Without MACE During Follow-Up

	Plaques in Patients With MACE (n = 49)	Plaques in Patients Without MACE (n = 439)	p Value
Radiofrequency IVUS*			
Plaque area, mm^2	10.0 (8.4–11.6)	8.2 (7.7–8.8)	0.03
Dense calcium, %	6.3 (5.7–7.0)	5.4 (2.8–8.0)	0.51
Necrotic core, %	12.4 (10.2–14.5)	12.9 (12.1–13.7)	0.64
Fibrous tissue, %	32.6 (28.4–36.8)	29.7 (28.4–31.0)	0.19
Fibrofatty tissue, %	10.3 (7.9–12.6)	6.8 (6.1–7.6)	<0.01
VH plaque classification			
TCFA	11 (22)	100 (22)	0.73
CTFA	22 (45)	191 (43)	0.49
NCTFA	16 (33)	148 (35)	0.76
Palpography			
Maximum strain value (endpoint #1), %	0.51 ± 0.38	0.57 ± 0.43	0.409
	0.40 (0.20–0.80)	0.50 (0.30–0.70)	
Density of ROC III–IV (endpoint #2), ROC/mm	0.06 ± 0.20	0.09 ± 0.22	0.399
	0.00 (0.00–0.00)	0.00 (0.00–0.00)	
Density of ROC I–IV (endpoint #3), ROC/mm	0.30 ± 0.23	0.33 ± 0.26	0.420
	0.29 (0.13–0.51)	0.25 (0.15–0.41)	

Values are n (%), mean ± SD, or median (interquartile range). *These values are presented as generalized estimating equation–adjusted least mean square (95% confidence interval).
MACE = major adverse cardiac event; VH = virtual histology; other abbreviations as in Tables 3 and 4.

the C-reactive protein values, as found in a previous study (18).

It is important to highlight that the strain values of palpography were lower in our population compared with previous studies (8,27); these low strain values may be the reason for the low rates of cardiac events recorded in our population. Palpography can, indeed, potentially identify some of the mechanical properties of coronary plaques that are more prone to rupture and lead to a clinical event such as cardiac death or acute myocardial infarction (18,19). However, during the follow-up, no patients experienced either cardiac death or myocardial infarction, only progressive stable or unstable angina. For these reasons, our study, therefore, may have been underpowered to detect possible differences in the mechanical properties of coronary plaques more prone to cause serious cardiac events (cardiac death, cardiac arrest, or myocardial infarction). The low rate of events confirms the results of the main trial in which the 3-year rate of serious adverse events was 4.9%, attesting to the favorable outcomes that may be achieved in this population with high compliance with medical therapy and close clinical follow-up (9).

Study limitations. The main limitations are the small sample size and the low event rate at follow-up. IVUS has an axial resolution of ~100 to 200 μm, whereas the pathologic definition of TCFA typically requires a cap thickness <65 μm (3). As such, a proportion of the lesions classified as TCFAs by radiofrequency IVUS were more likely to have had thick fibrous caps. At present, no data are available to show that that IVUS-VH could be used to make treatment decisions.

CONCLUSIONS

Our data confirm that larger fibroatheromas occur more frequently in patients in whom cardiac events develop during long-term follow-up, although no statistical differences in VH plaque classification were found between patients with or without MACE. However, a combined approach by IVUS-VH and palpography did not lead to any additional information with regard to aiding diagnostic identification of the fibroatheroma with the higher risk of rupture. In light of these results, the future application of palpography as an intracoronary imaging device to detect high-risk lesions needs to be revisited.

Reprint requests and correspondence: Dr. Patrick W. Serruys, Thoraxcenter, Ba-583, 's Gravendijkwal 230, 3015 CE Rotterdam, the Netherlands. *E-mail: p.w.j.serruys@erasmusmc.nl.*

REFERENCES

1. Ambrose JA, Tannenbaum MA, Alexopoulos D, et al. Angiographic progression of coronary artery disease and the development of myocardial infarction. J Am Coll Cardiol 1988; 12:56–62.
2. Glaser R, Selzer F, Faxon DP, et al. Clinical progression of incidental, asymptomatic lesions discovered during culprit vessel coronary intervention. Circulation 2005;111:143–9.
3. Virmani R, Burke AP, Farb A, Kolodgie FD. Pathology of the vulnerable plaque. J Am Coll Cardiol 2006;47:C13–8.
4. Naghavi M, Libby P, Falk E, et al. From vulnerable plaque to vulnerable patient: a call for new definitions and risk assessment strategies: part II. Circulation 2003;108:1772–8.
5. Naghavi M, Libby P, Falk E, et al. From vulnerable plaque to vulnerable patient: a call for new definitions and risk assessment strategies: part I. Circulation 2003;108:1664–72.
6. Schaar JA, Muller JE, Falk E, et al. Terminology for high-risk and vulnerable coronary artery plaques. Report of a meeting on the vulnerable plaque, June 17 and 18, 2003, Santorini, Greece. Eur Heart J 2004;25: 1077–82.
7. Loree HM, Kamm RD, Stringfellow RG, Lee RT. Effects of fibrous cap thickness on peak circumferential stress in model atherosclerotic vessels. Circ Res 1992;71:850–8.
8. Rodriguez-Granillo GA, Garcia-Garcia HM, Valgimigli M, et al. In vivo relationship between compositional and mechanical imaging of coronary arteries. Insights from intravascular ultrasound radiofrequency data analysis. Am Heart J 2006;151: 1025.e1–6.
9. Stone G, Maehara A, Lansky AJ, et al. A prospective natural-history study of coronary atherosclerosis. N Engl J Med 2011;364:226–35.
10. Maehara A, Cristea E, Mintz GS, et al. Definitions and methodology for the grayscale and radiofrequency intravascular ultrasound and coronary angiographic analyses. J Am Coll Cardiol Img 2012;5 Suppl S:S1–9.
11. Marso SP, Mercado N, Maehara A, et al. Plaque composition and clinical outcomes in acute coronary syndrome patients with metabolic syndrome or diabetes. J Am Coll Cardiol Img 2012;5:Suppl S:42–52.
12. Baber U, Stone GW, Weisz G, et al. Coronary plaque composition, morphology and outcomes in patients with and without chronic kidney disease presenting with acute coronary syndromes. J Am Coll Cardiol Img 2012;5:Suppl S:S53–61.
13. Lansky AJ, Ng VG, Maehara A, et al. Gender and the extent of coronary atherosclerosis, plaque composition and clinical outcomes in acute coronary syndromes. J Am Coll Cardiol Img 2012;5 Suppl S:S62–72.
14. McPherson JA, Maehara A, Weisz G, et al. Residual plaque burden in patients with acute coronary syndromes after successful percutaneous coronary intervention: extent, characterization, and clinical implications. J Am Coll Cardiol Img 2012;5 Suppl S:S76–85.
15. Brener SJ, Mintz GS, Cristea E, et al. Characteristics and clinical significance of angiographically mild lesions in acute coronary syndromes. J Am Coll Cardiol Img 2012;5 Suppl S:S86–94.
16. Sanidas EA, Mintz GS, Maehara A, et al. Adverse cardiovascular events arising from atherosclerotic lesions with and without angiographic disease progression. J Am Coll Cardiol Img 2012;5 Suppl S:S95–105.
17. Schaar JA, De Korte CL, Mastik F, et al. Characterizing vulnerable plaque features with intravascular elastography. Circulation 2003;108:2636–41.
18. Schaar JA, Regar E, Mastik F, et al. Incidence of high-strain patterns in human coronary arteries: assessment with three-dimensional intravascular palpography and correlation with clinical presentation. Circulation 2004; 109:2716–9.
19. Schaar JA, van der Steen AF, Mastik F, Baldewsing RA, Serruys PW. Intravascular palpography for vulnerable plaque assessment. J Am Coll Cardiol 2006;47:C86–91.
20. Nair A, Kuban BD, Tuzcu EM, Schoenhagen P, Nissen SE, Vince DG. Coronary plaque classification with intravascular ultrasound radiofrequency data analysis. Circulation 2002;106:2200–6.
21. Nair A, Margolis MP, Kuban BD, Vince DG. Automated coronary plaque characterisation with intravascular ultrasound backscatter: ex vivo validation. EuroIntervention 2007;3: 113–20.
22. Garcia-Garcia HM, Mintz GS, Lerman A, et al. Tissue characterisation using intravascular radiofrequency data analysis: recommendations for acquisition, analysis, interpretation and reporting. EuroIntervention 2009;5:177–89.
23. Rodriguez-Granillo GA, Garcia-Garcia HM, Mc Fadden EP, et al. In vivo intravascular ultrasound-derived thin-cap fibroatheroma detection using ultrasound radiofrequency data analysis. J Am Coll Cardiol 2005;46: 2038–42.
24. Garcia-Garcia HM, Goedhart D, Serruys PW. Relation of plaque size to necrotic core in the three major coronary arteries in patients with acute coronary syndrome as determined by intravascular ultrasonic imaging radiofrequency. Am J Cardiol 2007;99: 790–2.
25. Qian J, Maehara A, Mintz GS, et al. Relation between individual plaque components and overall plaque burden in the prospective, multicenter virtual histology intravascular ultrasound registry. Am J Cardiol 2009;104:501–6.
26. de Korte CL, Sierevogel MJ, Mastik F, et al. Identification of atherosclerotic plaque components with intravascular ultrasound elastography in vivo: a Yucatan pig study. Circulation 2002;105:1627–30.
27. Serruys PW, Garcia-Garcia HM, Buszman P, et al. Effects of the direct lipoprotein-associated phospholipase A(2) inhibitor darapladib on human coronary atherosclerotic plaque. Circulation 2008;118:1172–82.

Key Words: intravascular ultrasound ■ palpography.